Isotopic fractionation of carbon during uptake by phytoplankton across the South Atlantic subtropical convergence

Robyn E. Tuerena[1], Raja S. Ganeshram[1], Matthew P. Humphreys[2†], Thomas J. Browning[3‡], Heather Bouman[3], and Alexander. P. Piotrowski[4],

[1]School of GeoSciences, University of Edinburgh, Edinburgh, UK
[2]Ocean and Earth Science, University of Southampton, Southampton, UK
[3]Department of Earth Sciences, University of Oxford, Oxford, UK
[4]School of Geosciences, University of Cambridge, Cambridge, UK

[†] Now at: School of Environmental Sciences, University of East Anglia, Norwich, UK
[‡] Now at: GEOMAR Helmholtz Centre for Ocean Research, Kiel, Germany

Correspondence to: Robyn E. Tuerena (r.tuerena@ed.ac.uk)

Abstract. The stable isotopic composition of particulate organic carbon ($\delta^{13}C_{POC}$) in the surface waters of the global ocean can vary with the aqueous CO_2 concentration ($[CO_{2(aq)}]$) and affects the trophic transfer of carbon isotopes in the marine food web. Other factors such as cell size, growth rate and carbon concentrating mechanisms decouple this observed correlation. Here, the variability in $\delta^{13}C_{POC}$ is investigated in surface waters across the south subtropical convergence (SSTC) in the Atlantic Ocean, to determine carbon isotope fractionation (ε_p) by phytoplankton and the contrasting mechanisms of carbon uptake in the subantarctic and subtropical water masses. Our results indicate that cell size is the primary determinant of $\delta^{13}C_{POC}$ across the Atlantic SSTC in summer. Combining cell size estimates with CO_2 concentrations, we can accurately estimate ε_p within the varying surface water masses in this region. We further utilize these results to investigate future changes in ε_p with increased anthropogenic carbon availability. Our results suggest that smaller cells, which are prevalent in the subtropical ocean, will respond less to increased $[CO_{2(aq)}]$ than the larger cells found south of the SSTC and in the wider Southern Ocean. In the subantarctic water masses, isotopic fractionation during carbon uptake will likely increase, both with increasing CO_2 availability to the cell, but also if increased stratification leads to decreases in average community cell size. Coupled with decreasing $\delta^{13}C$ of $[CO_{2(aq)}]$ due to anthropogenic CO_2 emissions, this change in isotopic fractionation and lowering of $\delta^{13}C_{POC}$ may propagate through the marine food web, with implications for the use of $\delta^{13}C_{POC}$ as a tracer of dietary sources in the marine environment.

1 Introduction

The marine environment is undergoing rapid changes as atmospheric carbon dioxide increases, with the greatest change occurring in the upper ocean (Gruber et al., 1999; Sabine and Tanhua, 2010). Anthropogenic carbon inputs and the increase of greenhouse gases in the atmosphere are causing ocean warming (Cheng et al., 2019), changes to upper ocean stratification (Bopp et al., 2001; Capotondi et al., 2012) and altered distributions of nutrients and carbon (Khatiwala et al., 2013; Quay et al., 2003; Gruber et al., 2019). Marine phytoplankton are diverse, and are already responding to ocean warming, including changes to productivity (Behrenfeld et al., 2006, Arrigo and van Dijken, 2015), the length of growing season (Henson et al., 2018) and phytoplankton cell size (Finkel et al., 2010). Alterations to phytoplankton diversity and/or productivity will likely have knock-on effects on marine food web dynamics. Investigating such changes in the remote marine environments requires tracers that can pinpoint shifts in dietary sources. The $\delta^{13}C$ of organic carbon in marine plants and animals can provide information on carbon sources to the base of the food web (Peterson and Fry, 1987, Post, 2002). Improved understanding of ^{13}C systematics will lead to reliable use of this proxy in future predictions.

During photosynthesis, marine phytoplankton take up aqueous CO_2 ($[CO_{2(aq)}]$) and convert it into organic carbon. In this process the lighter isotope (^{12}C) is preferentially consumed, leaving the residual aqueous pool increasingly enriched in the heavier isotope. The stable carbon isotopic composition of marine phytoplankton is determined by the uptake fractionation (ε_p), which is influenced by ambient environmental conditions and phytoplankton cell physiology. Therefore the $\delta^{13}C$ of marine plankton can indicate the controlling mechanisms behind carbon uptake which led to its use as a potential proxy to reconstruct surface water $[CO_{2(aq)}]$ of past climates (Freeman and Hayes, 1992, Jasper et al., 1994).

The $\delta^{13}C$ of particulate organic carbon ($\delta^{13}C_{POC}$) varies over relatively large oceanic areas and has been found to inversely correlate with $[CO_{2(aq)}]$ (the principal carbon source) in surface waters (Rau et al., 1991; Sackett et al., 1965). High $[CO_{2(aq)}]$ can lead to greater discrimination against ^{13}C as the light isotope is preferentially consumed by phytoplankton. The low temperature waters of the Southern Ocean and their high $[CO_{2(aq)}]$ lead to negative $\delta^{13}C$ excursions in marine plankton there (Sackett et al., 1964). Although this relationship holds true to first order over global datasets (Rau et al., 1989), in many marine environments the local variability in $\delta^{13}C_{POC}$ can be attributed to other mechanisms.

Phytoplankton growth rate, cell size and cell geometry are also important controls on $\delta^{13}C_{POC}$ in surface waters (Bidigare et al., 1997; Francois et al., 1993; Popp et al., 1998; Laws et al., 1995; Villinski et al., 2000). These ecophysiological factors decouple the observed relationship between $\delta^{13}C_{POC}$ and $[CO_{2(aq)}]$, limiting the reliability of $\delta^{13}C_{POC}$ as a palaeoproxy. This is particularly true in areas where $[CO_{2(aq)}]$ is lower or less variable, as other factors have been found to be more important for determining the degree of isotopic fractionation (Henley et al., 2012; Lourey et al., 2004; Popp et al., 1998). In field studies, smaller sized phytoplankton have been measured with lower $\delta^{13}C_{POC,}$ compared to larger cells such as diatoms, particularly in fast growing blooms (Hansman and Sessions, 2015, Rau et al., 1990). These findings indicate that the factors determining $\delta^{13}C_{POC}$ may vary as you transition contrasting marine environments.

The carbon fixation pathway can vary amongst phytoplankton species through the assimilation of bicarbonate via active transport as opposed to diffusive CO_2 uptake. In general, more negative excursions in $\delta^{13}C_{POC}$ are associated with diffusive entry of CO_2, whereas CCMs or diffusive limitation of carbon supply lead to more positive $\delta^{13}C_{POC}$ (Raven et al., 2008). When $[CO_{2(aq)}]$ falls below a critical level, the active transport of CO_2 into the cell can enrich $\delta^{13}C_{POC}$, but this has been found to be proportional to carbon demand or growth rate (Popp et al., 1998). CCMs occur in most cyanobacteria, increasing CO_2 at the site of Rubisco activity (Raven et al., 2008).

All of the processes which alter the uptake fractionation of $[CO_{2(aq)}]$ will ultimately determine the isotopic variability in carbon at the base of the marine food web. Thus, the factors that are sensitive to ongoing climate change need to be better understood in order to accurately use $\delta^{13}C_{POC}$ as a tracer of dietary sources and in food web studies.

In this study we investigate the mechanisms for isotopic fractionation in $\delta^{13}C_{POC}$ resulting from carbon uptake and biological production in the upper ocean. We report data from a full transect across the south subtropical convergence (SSTC) in the Atlantic basin, which captures a region of productive open ocean. The cruise sampled both subantarctic and subtropical regimes with contrasting limiting nutrient environments and community structure (Browning et al., 2014). The parameters $[CO_{2(aq)}]$ and $\delta^{13}C_{DIC}$, together with chlorophyll-a and other diagnostic phytoplankton pigments are used collectively to disentangle the processes which fractionate $\delta^{13}C_{POC}$ as a response to algal uptake of $[CO_{2(aq)}]$ across this region. We find the community cell size, as estimated using phytoplankton pigment composition, to be the primary determinant of $\delta^{13}C_{POC}$ across the SSTC, with smaller cell sizes increasing the carbon availability for fixation. The results from the field study are used to understand/infer how $\delta^{13}C_{POC}$ in this region may change into the future with ongoing climate change.

2. Methods

2.1 Carbon concentrations and isotopic measurements

Samples were collected onboard the RRS James Cook between December 2011 and February 2012 (JC068), as part of the GEOTRACES A10 transect of the South Atlantic. An east to west transect was conducted with upper ocean sampling at each station. Standard CTD measurements and water sampling were performed using a stainless steel rosette equipped with a full sensor array and 24×20-litre OTE bottles. Salinity, temperature and depth were measured using a CTD system (Seabird 911+) and salinity was calibrated on-board with discrete samples using an Autosal 8400B salinometer (Guildline).

Measurements of total CO_2 (TCO_2) and total alkalinity (TA) were carried out at sea within 24 hours of collection. Samples were warmed in a water bath at 25 °C for an hour before analysis. A set volume of the sample is acidified by addition of excess 10% phosphoric acid, which converts all inorganic C species to CO_2. This is carried into the coulometric cell by an inert carrier gas (CO_2-free N_2 that is first passed through a magnesium perchlorate and Ascarite II scrubber), and a coulometric titration determines the amount of CO_2, which is equal to TCO_2. Small increments of 0.1 M hydrochloric acid are added to a separate subsample and the amount added to reach the carbonic acid equivalence point is equal to the TA (Humphreys, 2015). Regular measurements of both TCO_2 and TA were made from batch 114 Certified Reference Material (CRM) from A. G. Dickson

(Scripps Institution of Oceanography; Dickson et al., 2003) and used to calibrate the results. To obtain the final results in units of µmol kg^{-1}, a correction for density (ρ) due to salinity variation was then applied using salinity measured from Niskin bottle samples (Zeebe et al., 2001). Duplicate samples were taken from the same Niskin bottle and analysed consecutively.

[$CO_{2(aq)}$] was calculated from measured TA and DIC using CO2SYS v1.1 (Lewis and Wallace, 1998; van Heuven et al., 2011).

5 Equilibrium constants were evaluated following Mehrbach et al. (1973) for carbonic acid and Dickson (1990) for bisulfate, and we used the boron:chlorinity ratio of Lee et al. (2010).

Samples for the measurement of the stable isotopes of carbon in dissolved inorganic carbon ($\delta^{13}C_{DIC}$) were collected from the stainless steel rosette. Samples were taken into 250 mL glass bottles with ground glass stoppers. Water was drained directly into the sample bottle using silicone tubing to the bottom of the bottle to eliminate bubble formation. The bottle and cap were

10 rinsed once with water from the rosette bottle before overflowing the sample bottle by at least 1 bottle volume before withdrawing the silicone tube, carefully avoiding bubble formation. The stopper was then placed in the bottle and then removed so that 2.5 mL of sample could be removed to allow for thermal expansion, and 50 µL of 100% $HgCl_2$ added to halt any biological activity. The stoppers and the inside of the neck of the bottles were dried before the stopper, coated with vacuum grease, was replaced and secured with a foam insert and plastic cover. The samples were then shaken to disperse the $HgCl_2$

15 and stored at 4 °C until analysis. Samples were measured using a Thermo MAT253 stable isotope mass spectrometer. $\delta^{13}C_{CO2}$ was determined from $\delta^{13}C_{DIC}$ and absolute temperature (T_k), using $\delta^{13}C_{CO2} = \delta^{13}C_{DIC} + 23.644 - 9701.5/T_k$ (Rau et al., 1996). Particulate samples were collected onto ashed, pre-weighed GF/F microfibre filters (0.7 µm pore size, 25 mm diameter). Two to four litres of water were collected from the biological rosette in the surface 400 m depending on chlorophyll levels detected by the CTD fluorometer. The samples were pressure filtered simultaneously using an 8-way manifold system. Once the total

20 volume for each depth was filtered, the filters were extracted from the filter holder, placed in labelled aluminium foil and dried at 50 °C for ~12 hours. Once dried, filters were folded and stored in plastic sample bags at -20 °C. To remove carbonates prior to analysis, filters were wetted with Milli-Q water, fumed with 70% HCl for 48 hours in a desiccator, dried at 50 ºC and then folded into tin capsules. The filters were analysed using a Carlo Erba NA 2500 elemental analyser in-line with a VG PRISM III isotope ratio mass spectrometer for elemental POC/PN and $\delta^{13}C_{POC}$ and $\delta^{15}N_{PN}$. All $\delta^{13}C_{POC}$ data presented in this study are

25 in the delta per mil notation versus V-PDB (‰ VPDB).

2.2 Cell size calculations

Phytoplankton pigments were analysed by High Pressure Liquid Chromatography (HPLC) analysis. Between 500 and 2000 ml of seawater was filtered through 25 mm GF/F filters. The filters were placed in 2 ml cryovials and flash frozen in liquid

30 nitrogen. Filters were then transferred to a -80°C freezer for longer term storage. Pigment extracts were analysed using a reverse-phase HPLC column using a Thermo Finnigan HPLC instrument at the National Oceanography Centre Southampton (Gibb et al., 2000). Phytoplankton pigments were extracted in 3 to 5 ml 90% acetone by ultrasonication and centrifugation. Extracts were loaded into a chilled autosampler prior to injection into the HPLC system. Pigments were detected by absorbance at 440 nm, and identified by diagnostic retention times. The resulting pigment assemblage was used to estimate the fractional

contribution of the three size classes (micro-, nano- and picophytoplankton) to total chlorophyll-a pigment concentration (Bricaud et al. 2004; Uitz et al. 2008).

3. Results

3.1 Oceanographic setting

The SSTC is characterised by the convergence of contrasting biogeochemical regimes. In the colder Subantarctic Surface Waters (SASW), located south of the SSTC, concentrations of macronutrients are elevated and primary production is primarily limited by iron availability (Browning et al., 2014). The subtropical waters to the north of the SSTC are associated with the South Atlantic subtropical gyre and are principally macronutrient limited, or possibly macronutrient-iron co-limited (Browning et al., 2014, 2017). The three subtropical water masses (Agulhas Current (AC), South Atlantic Central Water (SACW) and Brazil Current (BC)) can be readily identified with warmer temperatures and higher salinities, the influence of the Malvinas Current (MC) separates the core of the SACW and BC (Figure 1).

Higher $[CO_{2(aq)}]$ is associated with the lower temperatures of the SASW. Across the zonal transect, higher $\delta^{13}C_{CO2}$ is associated with lower $[CO2_{(aq)}]$ and warmer temperatures of the subtropical water masses (Figure 1). $\delta^{13}C_{CO2}$ is highest on the western boundary in the BC and in the Rio Plata outflow. $\delta^{13}C_{POC}$ across 40°S ranges from -25 to -20‰ indicating a predominantly marine source (e.g. Rau et al., 1989).

Satellite images of surface chlorophyll concentrations across this region indicate elevated standing stocks of phytoplankton in comparison to the South Atlantic gyre and subantarctic waters further south (Browning et al., 2014). Chlorophyll concentrations peak between austral spring and summer, and the south subtropical convergence (SSTC) moves south as a result of the expansion of the Agulhas and Brazil Currents. Depth profiles showed that the subantarctic waters have elevated and uniform chlorophyll concentrations (0.2-0.9 mg m^{-3}). Conversely in the subtropical waters a deep chlorophyll maximum is formed, with low surface concentrations of chlorophyll (<0.2 mg m^{-3}) and macronutrients (Tuerena et al., 2015).

3.2 $\delta^{13}C_{POC}$ variability

If $\delta^{13}C_{POC}$ is determined principally by changing ambient $[CO_{2(aq)}]$ and not influenced by cell physiology, such as growth rates and cell size the $\delta^{13}C_{POC}$ can often be predicted by sea surface temperature variability (Rau et al., 1989). In this study, $\delta^{13}C_{POC}$ is compared to a model from Rau et al. (1996), which predicts the carbon isotope fractionation (ε_p) and $\delta^{13}C_{POC}$ where photosynthesis is strictly based on the passive diffusion of CO_2 into marine phytoplankton cells.

Modelled $\delta^{13}C_{POC}$ was calculated using the diffusion model of Rau et al. (1996), where

$$\delta^{13}C_{POC} = \delta^{13}C_{CO2} - \varepsilon_f + (\varepsilon_f - \varepsilon_d)\frac{Q_s}{[CO_{2(aq)}]}\left(\frac{r}{D_T\left(1+\frac{r}{r_k}\right)} + \frac{1}{P}\right), \tag{1}$$

where ε_f = intracellular enzymatic isotope fractionation (‰), ε_d = Diffusive isotope fractionation of $CO_{2(aq)}$ in seawater (‰), Q_s = CO_2 uptake rate per unit cell surface area (mol-C m^{-2} s^{-1}), $[CO_{2(aq)}]$= ambient $CO_{2(aq)}$ concentration (mol m^{-3}), r = cell radius (m), D_T = temperature dependent diffusion rate of CO_2 (m^2 s^{-1}), r_k = reacto-diffusive length (m) and P = cell wall permeability to CO_2 (m s^{-1}). Q_s was determined from

$$Q_s = \frac{(\gamma_c \, \mu_i)}{4\pi r^2} \tag{2}$$

where γ_c = carbon content per cell (mol-C), μ_i = cell growth rate (s^{-1}).

Using this model we tested how $\delta^{13}C_{POC}$ and ε_p vary as a function of $[CO_{2(aq)}]$, temperature, growth rate and cell size. For each of these parameters we used the base values of Rau et al. (1996) unless specified.

ε_p for measured and modelled $\delta^{13}C$ was calculated as:

$$\varepsilon_p = \delta^{13}C_{CO2} - \delta^{13}C_{POC} \tag{3}$$

To understand under what conditions the ambient $[CO_{2(aq)}]$ plays a dominant role in the determination of $\delta^{13}C_{POC}$ in surface waters across the frontal region, the relationships between $\delta^{13}C_{POC}$, $\delta^{13}C_{CO2}$, and $CO_{2(aq)}$ were compared to modelled estimates for passive diffusion (Figure 2). SASW samples fall close to the modelled estimates and subtropical samples decouple from the modelled trend to a much higher degree. In Figure 2a, $[CO_{2(aq)}]$ and $\delta^{13}C_{CO2}$ in the SASW have a significant negative correlation (r=-0.77, n=12, p=0.003), and correspond to the model trends, with lower concentrations resulting in higher $\delta^{13}C_{DIC}$ and $\delta^{13}C_{CO2}$. There are no significant correlations between $\delta^{13}C_{POC}$ and $[CO_{2(aq)}]$ or $\delta^{13}C_{CO2}$ in the subtropical or subantarctic water masses (Figure 2, p>0.05).These data suggest that although $[CO_{2(aq)}]$ may play a part in determining the $\delta^{13}C_{POC}$ in the SASW, other factors cause deviation away from a significant correlation, with the relationship increasingly decoupled in subtropical waters.

To investigate the spatial variability across the SSTC, $[CO_{2(aq)}]$, and $\delta^{13}C_{CO2}$ were plotted against longitude and compared to model estimates (Rau et al., 1996, supplementary information), where we used the model constants for cell size (10µm) and reconstructing $[CO_{2(aq)}]$ from temperature variability across the transect (Figure 3a and b). Temperature can predict the spatial variability in $[CO_{2(aq)}]$, and $\delta^{13}C_{CO2}$, however ambient $[CO_{2(aq)}]$ is lower and $\delta^{13}C_{CO2}$ higher than model estimates, resulting from biological production and the isotopic disequilibrium between the ocean and atmosphere (Gruber et al., 1997). $\delta^{13}C_{POC}$ is predicted using ambient temperature and also measurements of $[CO_{2(aq)}]$ and $\delta^{13}C_{CO2}$ (Figure 3c). There is no correlation between measured and modelled $\delta^{13}C_{POC}$ across the transect, suggesting there are other controlling factors which determine the $\delta^{13}C_{POC}$ variability.

To test whether cell size (and thus cellular surface area to volume ratio) plays an important role in determining $\delta^{13}C_{POC}$, we estimated the change in phytoplankton size classes across the transect. Using phytoplankton pigment data we calculated the relative proportion of pico-, nano- and microphytoplankton size fractions to total chlorophyll-a biomass (Bricaud et al. 2004; Uitz et al., 2008). Picophytoplankton were more abundant in the subtropical environments in comparison to the SASW,

contributing between 30-40% of the pigment biomass at the core of these water masses (Figure 4). In contrast, nano- and microphytoplankton were more dominant in the SASW and close to the Rio Plata outflow.

An estimate of the approximate average community cell size was calculated by defining a specific cell size for each of the three defined size classes (picophytoplankton=1 µm, nanophytoplankton=5 µm, microphytoplankton= 50 µm, Bricaud et al.

5 2004). The central size values for each class were divided by two to approximate the average community cell radius (picophytoplankton=0.5 µm, nanophytoplankton=2.5 µm, microphytoplankton= 25 µm). This method provides only a rough indicator of the community cell radius, as size class is being represented by one unique size for each algal group, however this enables one single parameter to be used to characterise the size structure of the algal population, which is important for the purposes of this study.

10 Estimated average cell radii were generally smaller at the core of the subtropical water masses compared to the SASW (Figure 5) (depth range <40 m, subtropical [>20 °C] 6.5 µm ±0.8, n=17, subantarctic [<18 °C] 10.4 µm ±2.3, n=31). Increasing the average cell size (and thus decreasing SA:V) has the potential to reduce carbon isotope fractionation during uptake by passive diffusion and thus increase $\delta^{13}C_{POC}$, by reducing the ability of the cell to discriminate between the two isotopes. This has been found in modelled, experimental and environmental studies (Popp et al., 1998, Pancost et al., 1997, Rau et al., 1990, 1996).

15 When $\delta^{13}C_{POC}$ is modelled using temperature, SASW measurements fall between model estimates for a cell radius of 10-15 µm (Figure 6a). Conversely, the subtropical samples have higher proportions of picoplankton (<2 µm), and decrease to lower $\delta^{13}C_{POC}$ than those predicted using temperature alone, demonstrating that cell size is likely a controlling factor in $\delta^{13}C_{POC}$ determination. The average community cell radius in open ocean samples were compared to $\delta^{13}C_{POC}$ (Figure 6b), and a significant positive correlation was observed size (r=0.74, n=30, p<0.001).

20 The samples with a larger estimated community cell size on both the east and western margins were not included in this correlation analysis as they show a significant offset from this relationship (Figure 6b). These samples have a larger estimated cell size compared to measured $\delta^{13}C_{POC}$ and suggest there is a possible terrestrial influence, either with the supply of allochthonous material, the presence of grazers and/or significant shifts in species assemblage to a higher abundance of micro plankton (Browning et al., 2014). The significant positive correlation between cell size and $\delta^{13}C_{POC}$ for open ocean waters

25 suggests that cell size is the primary factor influencing $\delta^{13}C_{POC}$ in the surface waters across the SSTC. We further test the relationship between $\delta^{13}C_{POC}$ and cell size by predicting changes in $\delta^{13}C_{POC}$ using temperature and cell size measurements (black crosses in Figure 6b). We find good agreement between modelled and measured data points, demonstrating the importance of cell size in estimating $\delta^{13}C_{POC}$.

South of the SSTC, the phytoplankton community is dominated by haptophytes (Browning et al., 2014). A lower species

30 diversity south of the front may explain the closer alignment between $[CO_{2(aq)}]$ and $\delta^{13}C_{POC}$, as other factors are less significant in influencing ε_p. Recent work has highlighted the interspecies differences in carbon uptake fractionation and their influence on bulk $\delta^{13}C_{POC}$ (Hansman and Sessions, 2016). Our results suggest a changing community cell size deviates $\delta^{13}C_{POC}$ from expected trends with $[CO_{2(aq)}]$. In this open ocean environment, using estimates of cell size in addition to $[CO_{2(aq)}]$, we can predict variability in $\delta^{13}C_{POC}$.

4. Discussion

4.1 Carbon uptake fractionation across the 40°S transect

The biological fractionation of carbon isotopes during uptake by phytoplankton can be estimated using $\varepsilon_p \sim \delta^{13}C_{CO2} - \delta^{13}C_{POC}$ (Freeman and Hayes, 1992). This fractionation comprises both the CO_2 fixation during photosynthesis, which utilizes the enzyme Rubisco ($\sim$-22 to -31‰), and is also determined by the factors which limit the external supply of CO_2 to the enzyme. Therefore, the more CO_2-limited the cell, the less the isotopic fractionation of CO_2 fixation will be expressed. These limiting factors include ambient $[CO_{2(aq)}]$ (Baird et al., 2001), growth rates (Laws et al., 1995, Popp et al 1998), cell size or geometry (Popp et al., 1998), light availability and day length (Laws et al., 1995, Burkhardt et al., 1995), utilization of HCO_3^- in replacement of CO_2 (Sharkey and Berry, 1985) and species variability (Falkowski, 1991).

Empirical estimates of ε_p range between 10-18‰, with the highest fractionation observed in the Southern Ocean where $[CO_{2(aq)}]$ is highest, increasing to over 20 μM in surface waters (Young et al., 2013). Over the Atlantic SSTC we measure an ε_p range of 12-17 ‰. In the subtropical water masses north of the SSTC, the average ε_p is 1 ‰ higher than in the SASW despite lower $[CO_{2(aq)}]$ (Figure 7). Our data contrast the global observed variability (of high ε_p in high $[CO_{2(aq)}]$ regions such as the Southern Ocean) but are comparable to results from previous work in frontal regions where higher ε_p has been observed in lower $[CO_{2(aq)}]$ subtropical water masses (Bentaleb et al., 1998, Francois et al., 1993).

We predict the variability in ε_p using temperature, $[CO_{2(aq)}]$, $\delta^{13}C_{CO2}$ and changes in community cell size across the region. If $[CO_{2(aq)}]$ was the controlling mechanism behind ε_p, increases in $[CO_{2(aq)}]$ would result in increased ε_p. There is no significant trend between modelled ε_p (temperature, $[CO_{2(aq)}]$) and measured ε_p (Figure 7a). In contrast, when cell size is included, there is a significant positive correlation (Figure 7c, r=0.72, p=0, df=18). These results indicate that in this region, there is an inverse trend between modelled ε_p and $[CO_{2(aq)}]$: ε_p increases with decreasing $[CO_{2(aq)}]$, which can be best attributed to the variability in the gross size structure of the phytoplankton assemblage across the SSTC (Figure 7).

If the flow of $[CO_{2(aq)}]$ into and out of a cell is determined by gas diffusion, then the flow is proportional to the cell surface area. A decrease in cell radius leads to an increase in cell surface area to volume ratio (SA:V), increasing the amount of $[CO_{2(aq)}]$ diffusing across the cell membrane relative to the total carbon within the cell, and allowing greater fractionation and higher ε_p. Thus ε_p has been found to be negatively correlated to phytoplankton cell size, with larger cells such as diatoms showing less isotopic fractionation compared to smaller phytoplankton (Popp et al., 1998, Hansman and Sessions, 2016). These cell size trends are observed across our open ocean transect, with the largest cell sizes having lower ε_p and higher $\delta^{13}C_{POC}$.

The influence of cell size on the expression of ε_p is likely to have a greater effect with increasing growth rate (Rau et al., 1996, Popp et al., 1998). A higher growth rate, such as in spring/summer blooms increases the range in ε_p expressed across cell sizes. For instance in fast growing blooms, larger cell sizes may have higher relative $\delta^{13}C_{POC}$ and lower ε_p than smaller cell sizes, compared to in low growth periods (e.g. Fry and Wainwright, 1991). The SSTC is a dynamic nutrient environment (Ito et al 2005), with the convergence of N limited subtropical waters (Eppley et al., 1979), with the iron limited ACC waters (Boyd et

al., 2000, Browning et al., 2014). The convergence of contrasting regimes potentially increases nutrient availability to phytoplankton whilst also contributing to thermal stability of the upper water column (Longhurst, 1998), thus having the potential to elevate growth rates. Therefore the expression of cell size on ε_p is intuitive in this environment. An increase in ε_p with decreasing cell size has been noted in previous work (Goericke and Fry, 1994) and may be the primary driver for community ε_p in the SSTC during spring and summer, when growth rates are high.

4.2 Regional and global factors influencing uptake fractionation

The changing $[CO_{2(aq)}]$ is the principal determinant of $\delta^{13}C_{POC}$ across the global ocean (Sackett et al., 1965; Rau et al., 1989; Goericke and Fry, 1994). A modelling study found that the inter-hemispheric differences in $\delta^{13}C_{POC}$ could be explained by the inter-hemispheric asymmetry in $[CO_{2(aq)}]$ (Hofmann et al., 2000). Poleward of ~50°S, $[CO_{2(aq)}]$ ranges between 15-25 µM, $\delta^{13}C_{POC}$ between -30 and -24 ‰ and ε_p is greatest of anywhere in the global ocean (Figure 8). The fractionation during carbon fixation (Rubisco) is highly expressed on ε_p and other factors are less influential.

In the low latitude ocean, previous studies have shown that this trend becomes decoupled: $[CO_{2(aq)}]$ decreases, growth rates are more variable and community structure and seasonal dynamics decouple the observed correlation of fractionation with temperature (e.g. Francois et al., 1993, Bentaleb et al., 1998). Previous studies of ε_p at the SSTC found decoupling between $\delta^{13}C_{POC}$ and $[CO_{2(aq)}]$, attributed to changing physical processes across the frontal region (Francois et al., 1993, Bentaleb et al., 1998). The variable water mass movements decouple trends and it has been suggested that $\delta^{13}C_{POC}$ variability in water masses can result from the local phytoplankton assemblage (Fontugne and Duplessy, 1978). Strong seasonal variations in $\delta^{13}C_{POC}$ can also result from changes in biological parameters such as cell radius, cell membrane permeability and growth rate (Francois et al., 1993; Goericke and Fry, 1994; Jasper et al., 1994; Laws et al., 1995; Popp et al., 1998). Phytoplankton assemblage-derived changes in ε_p have been observed in other changing environments, such as the Seasonal Sea Ice Zone (Dehairs et al., 1997; Popp et al., 1999) and in major frontal regions (Dehairs et al., 1997; Popp et al., 1999; this study).

The results from our field study demonstrate that the phytoplankton assemblage has a key role in determining ε_p and $\delta^{13}C_{POC}$ from their cell size and physiology, likely linked to the high growth rates in this frontal region. We test whether cell size variability presents a control over ε_p across meridional transects (Figure 8). We find no relatable trend on a global scale and latitudinal trends demonstrate an increase in ε_p with an increase in $[CO_{2(aq)}]$. However increased cell size reduces the expression of a high ε_p (as shown with the higher $\delta^{13}C_{POC}$ and lower ε_p in Figure 8c and d), which is particularly evident between 30-60°S. Thus, regions where frequent physical changes stimulate variable and diverse phytoplankton assemblages may be more likely to have a decoupled relationship between ε_p and $[CO_{2(aq)}]$. We suggest that the high growth rates across this region play an important role in driving this change – we sampled across the SSTC in summer (high light levels), which may further promote the importance of cell size in determining $\delta^{13}C_{POC}$.

4.3 Changes to uptake fractionation and $\delta^{13}C_{POC}$ in response to climate change

Ambient $[CO_{2(aq)}]$ is increasing in the global ocean. A recent study found that ϵ_p has increased significantly since the 1960s in the subtropical Atlantic, whereas no notable change has been detected in polar regions (Young et al., 2013). Our results suggest that a change in the community cell size would impact ϵ_p, with a decrease in cell radius leading to increased ϵ_p. Thus, a changing

5   community structure with the onset of climate change may further impact the ϵ_p and $\delta^{13}C_{POC}$, and have implications to our understanding of carbon isotope variability at the base of the food web.

Observational studies show rapid warming in the world's oceans in response to climate change, and that most of the ocean heat uptake is stored in the upper 75 m (Cheng et al, 2019). Predicted ocean warming trends are variable in different regions, with a greater rate of increase predicted in the polar regions (IPCC, 2010). Warming at the ocean surface promotes thermal

10   stratification, which, in the Southern Ocean may decrease light limitation, whereas in the subtropics is likely to promote further nutrient limitation (Sarmiento et al., 2004). Thus, climate change will promote varying responses from phytoplankton communities and their physiology across the global ocean (Rousseaux and Gregg, 2015).

In the oligotrophic gyres, ocean-atmosphere GCMs project increased stratification and decreases in net primary productivity with the onset of climate change (Boyd and Doney, 2002; Capotondi et al., 2012; Le Quere et al., 2003). Nutrients are already

15   the limiting factor for net primary productivity and small cells are readily adapted to these oligotrophic environments, where recycled nutrients such as ammonium are the main nutrients available to phytoplankton (Fawcett et al., 2011). Many studies observe a shift to phytoplankton communities dominated by picoplankton as the water column becomes stratified and increasingly nutrient depleted (Atkinson et al., 2003; Bouman et al., 2003; Latasa and Bidigare, 1998; Lindell and Post, 1995; Irwin and Oliver 2009). These observations suggest that the average community cell size may decrease further with ongoing

20   climate change.

There may be large scale shifts in community structure, including the physiological dependencies of phytoplankton on light and nutrients and their ecological diversity (Bouman et al., 2005; Behrenfeld et al., 2005; Siegel et al., 2005). A decrease in cell size may lead to a faster pace of metabolism (Brown et al., 2004). However, recent work suggests that CO_2 fixation and respiration rates are unlikely to increase under nutrient limiting conditions (Maranon et al., 2018). Therefore subtropical

25   regions may simultaneously experience warming, decreases in nutrient supply, increases in CO_2 availability, decreases in cell size and changes to community structure.

At higher latitudes, models predict increases in net primary production with improved light availability in the mixed layer and an extended growing season (Bopp et al., 2001, Sarmiento et al 2004). Warming and reduction in sea ice is likely to initiate an earlier onset of bloom with a predicted 5-10 days shift per decade (Henson et al., 2018). Therefore, in the subantarctic ocean

30   we may expect decreased light limitation, higher growth rates and decreases in community cell size. The results from this study demonstrate the different physiology of phytoplankton across the SSTC and the expression of carbon uptake on $\delta^{13}C$ fixed into the phytoplankton cell. We find that $\delta^{13}C_{POC}$ can be predicted using variability in cell size and $[CO_{2(aq)}]$. Further to

this, the subtropical and subantarctic uptake fractionation may respond differently with changing ambient $[CO_{2(aq)}]$ and temperature with predicted future climate warming scenarios.

We use the results from this study to predict how the isotopic fractionation during carbon uptake may alter with increased $[CO_{2(aq)}]$ as a response to climate change. To do so, we alter the model inputs to increase atmospheric CO_2 from 400 ppm to

5 500 ppm, and thus increasing $[CO_{2(aq)}]$ in the surface ocean, which we calculate using the solubility coefficients of CO_2 in seawater (Figure 9, Weiss, 1974). We test variability from an average cell radius of 5, 10 and 20 μm and investigate the changes over the temperature range of the ocean. Although a smaller cell size (radius 5 μm) fractionates $\delta^{13}C$ to a greater degree than a larger cell, there is only a 1 ‰ increase in ε_p with a 100 ppm increase in atmospheric CO_2 concentrations (Figure 9a). Therefore changing CO_2 concentration alone may not have a large effect on $\delta^{13}C_{POC}$ in subtropical environments. Instead a

10 trend to smaller average cell size would have a much greater impact on the $\delta^{13}C_{POC}$ which is observed and predicted in the oligotrophic gyres.

In the subantarctic waters, although predicted ε_p is lower in the larger cell sizes expected south of the SSTC, an increase in ambient CO_2 concentrations would have a much larger effect on ε_p. There is an observed 3 ‰ increase in ε_p in larger phytoplankton (radius 20 μm) with a 100 ppm increase in atmospheric CO_2 concentration. The changing conditions in the

15 subantarctic ocean with the onset of climate change are also likely to promote the success of smaller sized phytoplankton, as the light conditions improve and the upper ocean becomes increasingly stratified in summer months (Bopp et al., 2003). A decrease in community cell size could also increase ε_p and produce lower $\delta^{13}C_{POC}$. These results indicate that the subantarctic ocean, which has a relatively larger cell size in comparison to the subtropical ocean and is predicted to become increasingly stratified, may have a greater change in the $\delta^{13}C_{POC}$ produced during photosynthesis over the upcoming decades.

20 The sensitivity of $\delta^{13}C_{POC}$ to increases in anthropogenic carbon is determined by the change in $[CO_{2(aq)}]$ and also its isotopic signature. Enhanced diffusion of anthropogenic CO_2 between the atmosphere and the ocean's surface increases concentrations of $[CO_{2(aq)}]$ in the ocean (Friedli et al. 1986, Francey et al. 1999, Keeling et al. 2001). Anthropogenic CO_2 is enriched in the lighter ^{12}C isotope, so its invasion into the ocean decreases $\delta^{13}C_{DIC}$ in a phenomenon known as the Suess effect (Keeling, 1979), which has been observed across the ocean over the last decade (Quay et al. 2003). The uptake of anthropogenic CO_2 by

25 the world's oceans has led to a decrease in $\delta^{13}C_{DIC}$ by 0.025 % yr^{-1} (Gruber et al., 1999). The increase in seawater pCO$_2$ from 400 to 500 μatm shown in Figure 9 corresponds to DIC increasing by from 30 to 50 μmol kg^{-1} (with a greater DIC increase at higher temperatures). Assuming a ratio of anthropogenic CO_2 invasion to $\delta^{13}C_{DIC}$ change (i.e. ΔRC) of about −0.016 ‰ (μmol kg^{-1})$^{-1}$ in this region (Heimann and Maier-Reimer, 1996; McNeil et al., 2001), the associated Suess effect could decrease $\delta^{13}C_{DIC}$ – and therefore $\delta^{13}C_{POC}$ – by an extra 0.5 to 0.8 ‰, consistently across all cell sizes (Figure 9b). This decrease would

30 be additional to, and independent from, any change due to fractionation, and consistent in magnitude for every cell size.

Seawater warming, which is expected to accompany future increases in $[CO_{2(aq)}]$, independently modulates the marine carbonate system (Humphreys, 2017) and the fractionation model of Rau et al. (1996). In this case, simultaneous warming would oppose the increase in ε_p (and therefore decrease in $\delta^{13}C_{POC}$) driven by increasing $[CO_{2(aq)}]$, as shown by the negative

line gradients in Figure 9a (and positive gradients in Figure 9b). However, this is expected to have a relatively small impact overall, as the following back-of-the-envelope calculation illustrates. Given an equilibrium climate sensitivity (i.e. the equilibrium warming of Earth's near-surface resulting from a doubling of atmospheric pCO_2) of 1.5 to 4.5 °C (Stocker et al., 2013), an increase in pCO_2 from 400 to 500 ppm would drive from 0.5 to 1.5 °C of global mean warming. For 10 μm cells, the pCO_2 change alone would increase ε_p by ~1.8 ‰, while this warming alone would decrease ε_p by only 0.1 to 0.4 ‰, according to the model of Rau et al. (1996).

Stable isotope analysis of organic matter has emerged as the primary means for examining marine food web structure and variability (Middelburg, 2014). Carbon isotope signatures in particulate organic carbon vary substantially from the relative influence of terrestrial and marine carbon, carbon uptake pathways and the influence of carbon concentrating mechanisms (Jasper and Gagosian, 1990; Ganeshram et al., 1999). In contrast to nitrogen isotopes, there is negligible fractionation of carbon isotopes through trophic levels, which allows the accurate estimation of dietary sources of carbon (Minagawa and Wada, 1984). Therefore the factors which contribute to variability at the base of the food web need to be understood well in order to accurately understand marine food web dynamics (Peterson and Fry, 1987). These findings could also have implications to the distribution of $\delta^{13}C_{POC}$ in the deep ocean through organic matter sinking and burial (e.g. Cavagna et al., 2013).

This study highlights the importance of cell size as a primary determinant of the extent of isotopic fractionation in particulate organic carbon during uptake and the subsequent signature imparted at the base of the food web. Our findings support previous work predicting increases in ε_p and decreases in $\delta^{13}C_{POC}$ in the future (Young et al., 2013). Yet we suggest that increasing ε_p may predominantly result from shifts in community structure towards smaller sized phytoplankton. Changes in phytoplankton assemblages are being detected globally (Rousseaux and Gregg, 2015), in addition to possible declines in phytoplankton biomass (Boyce et al., 2010). Our detailed study of the subtropical and subantarctic environments predict greater relative decreases in $\delta^{13}C_{POC}$ in polar regions than in the subtropics in response to changing $[CO_{2(aq)}]$. If increased stratification proceeds in the subantarctic, this may also lead to decreases in average cell size and thus even greater decreases in $\delta^{13}C_{POC}$.

5. Conclusions

$\delta^{13}C_{POC}$ measurements from the SSTC in the Atlantic Ocean are compared to model predictions to determine the factors which control $\delta^{13}C$ variability and carbon uptake fractionation (ε_p). Our results contrast global trends in marine waters, where $\delta^{13}C_{POC}$ is lower in high CO_2 environments as a result of increased carbon uptake fractionation. Instead we find the $\delta^{13}C_{POC}$ and ε_p are largely determined by community cell size variability, which we estimate using phytoplankton pigment composition. We measured a greater ε_p in the subtropical water masses where smaller sized phytoplankton are more dominant and can fractionate $\delta^{13}C$ to a greater degree by the increased CO_2 availability to the enzyme rubisco as a result of their enhanced increase surface area to volume ratio. Our results suggest a greater variability in $\delta^{13}C$ and ε_p as a result of community cell size than previously predicted and highlight the need to understand the phytoplankton community structure.

We use our results from the field study to understand how increased CO_2 availability in the future will affect the carbon isotope fractionation in phytoplankton. Our findings suggest that larger celled phytoplankton in the subantarctic may respond more to changes in carbon concentration. However shifts in algal assemblages towards smaller phytoplankton will also have a large effect on the community ε_p expressed. These results suggest that decreasing cell size and increased CO_2 availability to phytoplankton will increase ε_p and decrease $\delta^{13}C_{POC}$. Our study illustrates that phytoplankton cell size changes in response to warming may alter $\delta^{13}C$ at base of the food chain, and need to be taken into account along with the Suess effect in using $\delta^{13}C$ as a food source tracer.

References

Arrigo, K. R., and van Dijken, G. L.: Continued increases in Arctic Ocean primary production, Prog. Oceanogr., 136, 60-70, doi: 10.1016/j.pocean.2015.05.002 , 2015.

5 Atkinson, D., Ciotti, B. J. and Montagnes, D. J. S.: Protists decrease in size linearly with temperature: ca. 2.5% degrees C-1, P. Roy. Soc. B-Biol. Sci., 270, 2605-2611, doi: 10.1098/rspb.2003.2538, 2003.

Baird, M. E., Emsley, S. M., and Mcglade, J. M., Using a phytoplankton growth model to predict the fractionation of stable carbon isotopes, Journal of Plankton Research, 23, 8, 841–848, doi: 10.1093/plankt/23.8.84, 2001.

Behrenfeld, M. J., Boss, E., Siegel, D. A., and Shea, D. M.: Carbon-based ocean productivity and phytoplankton physiology from space, Global Biogeochemical Cycles., 19,1, doi:10.1029/2004gb002299, 2005.

Behrenfeld, M. J., O'Malley, R. T., Siegel, D. A., McClain, C. R., Sarmiento, J. L., Feldman, G. C., Milligan, A. J., Falkowski,
15 P. G., Letelier, R. M., and Boss, E. S.: Climate-driven trends in contemporary ocean productivity, Nature 444, 752–755, doi:10.1038/nature05317, 2006.

Bentaleb, I., Fontugne, M., Descolas-Gros, C., Girardin, C., Mariotti, A., Pierre, C., Brunet, C., and Poisson, A.: Carbon isotopic fractionation by plankton in the Southern Indian Ocean: relationship between delta C-13 of particulate organic carbon
20 and dissolved carbon dioxide, J. Marine Syst., 17, 39-58, doi:10.1016/s0924-7963(98)00028-1, 1998.

Bidigare, R. R., Fluegge, A., Freeman, K. H., Hanson, K. L., Hayes, J. M., Hollander, D., Jasper, J. P., King, L. L., Laws, E. A., Milder, J., Millero, F.J., Pancost, R., Popp, B. N., Steinberg, P. A., Wakeham, S. G., Consistent fractionation of C-13 in nature and in the laboratory: Growth-rate effects in some haptophyte algae, Global Biogeochemical Cycles., 11, 279-292,
25 doi:10.1029/96gb03939, 1997.

Bopp, L., Monfray, P., Aumont, O., Dufresne, J. L., Le Treut, H., Madec, G., Terray, L., and Orr, J. C.: Potential impact of climate change on marine export production, Global Biogeochemical Cycles., 15, 81-99, doi: 10.1029/1999gb001256, 2001.

30 Bouman H.A., Platt, T., Sathyendranath, S., and Stuart, V: Dependence of light-saturated photosynthesis on temperature and community structure. Deep-Sea Res. I 52:1284-1299, 2005.

Bouman, H.A**.,** Platt, T., Sathyendranath, S., Li, W.K.W, Stuart, V., Fuentes Yaco, C., Maass, H., Horne, E.P.W., Ulloa, O., Lutz , V., and Kyewalyanga, M.: Temperature as an indicator of the optical properties and gross community structure of marine phytoplankton: implications for remote sensing of ocean colour. Mar. Ecol. Progr. Ser. 258:19-30, 2003.

5   Boyce, D.G., Lewis, M.R., and Worm, B.: Global phytoplankton decline over the past century. Nature, 466, 591-596, doi: 59110.1038/nature09268, 2010.

Boyd, P. W., Watson, A. J., Law, C. S., Abraham, E. R., Trull, T., Murdoch, R., Bakker, D. C. E., Bowie, A. R., Buesseler, K. O., Chang, H., Charette, M., Croot, P., Downing, K., Frew, R., Gall, M., Hadfield, M., Hall, J., Harvey, M., Jameson, G.,
10   LaRoche, J., Liddicoat, M., Ling, R., Maldonado, M. T., McKay, R. M., Nodder, S., Pickmere, S., Pridmore, R., Rintoul, S., Safi, K., Sutton, P., Strzepek, R., Tanneberger, K., Turner, S., Waite, A., and Zeldis, J.: A mesoscale phytoplankton bloom in the polar Southern Ocean stimulated by iron fertilization, Nature, 407, 695-702, 2000.

Boyd, P. W., and S. C. Doney, Modelling regional responses by marine pelagic ecosystems to global climate change,
15   Geophysical Research Letters, 29, 16, doi: 10.1029/2001gl014130, 2002.

Bricaud, A., Claustre, H., Ras, J., and Oubelkheir K.: Natural variability of phytoplanktonic absorption in oceanic waters: Influence of the size structure of algal populations, 109, C11010, doi:10.1029/2004JC002419, 2004

20   Brown, J. H., J. F. Gillooly, A. P. Allen, V. M. Savage, and G. B. West, Toward a metabolic theory of ecology, Ecology, 85, 1771-1789, doi:10.1890/03-9000, 2004.

Browning, T.J., Achterberg, E.P., Rapp, I., Engel, A., Bertrand, E.M., Tagliabue, A. and Moore, C.M.: Nutrient co-limitation at the boundary of an oceanic gyre. Nature, 551, 242, doi: 10.1038/nature24063, 2017.
25
Browning, T.J., Bouman, H. A., Moore, C. M., Schlosser, C., Tarran, G. A., Woodward, E. M. S., and Henderson, G. M., Nutrient regimes control phytoplankton exophysiology in the South Atlantic, Biogeosciences, 11, 463-479, doi:10.5194/bg-11-463-2014, 2014.

30   Burkhardt, S., Riebesell, U., and Zondervan, I.: Effects of growth rate, CO_2 concentration, and cell size on the stable carbon isotope fractionation in marine phytoplankton, Geochimica Et Cosmochimica Acta, 63, 3729-3741, doi:10.1016/s0016-7037(99)00217-3, 1999.

Capotondi, A., Alexander, M. A., Bond, N. A., Curchitser, E. N., and Scott, J. D.: Enhanced upper ocean stratification with climate change in the CMIP3 models, J. Geophys. Res. Oceans, 117, doi: 2012.

Cheng, L., Abraham, J., Hausfather, Z., and Trenberth, K. E.: How fast are the oceans warming? Science, 363, 128-129, doi: 10.1126/science.aav7619, 2019.

Cavagna, A.-J., Dehairs, F., Bouillon, S., Woule-Ebongué, V., Planchon, F., Delille, B., and Bouloubassi, I.: Water column distribution and carbon isotopic signal of cholesterol, brassicasterol and particulate organic carbon in the Atlantic sector of the Southern Ocean, Biogeosciences, 10, 2787-2801, https://doi.org/10.5194/bg-10-2787-2013, 2013.

Dehairs, F., Kopczynska, E., Nielsen, P., Lancelot, C., Bakker, D.C.E., Koeve, W., and Goeyens, L., δ^{13}C of Southern Ocean suspended organic matter during spring and early summer: regional and temporal variability, 44, 129-142, 1997.

Dickson, A. G., Afghan, J. D., and Anderson, G. C.: Reference materials for oceanic CO_2 analysis: a method for the certification of total alkalinity. Mar. Chem. 80, 185–197. doi: 10.1016/S0304-4203(02)00133-0, 2003.

Dickson, A. G.: Standard potential of the reaction: AgCl(s) + 0.5 H$_2$(g) = Ag(s) + HCl(aq), and the standard acidity constant of the ion HSO$_4^-$ in synthetic sea water from 273.15 to 318.15 K. J. Chem. Thermodyn. 22, 113–127. doi: 10.1016/0021-9614(90)90074-Z, 1990.

Falkowski, P. G., Ziemann, D., Kolber, Z., and Bienfang, P. K.: Role of eddy pumping in enhancing primary production in the ocean, Nature, 352, 55–58, doi: , 1991.

Farquhar, G. D., Oleary, M. H. , and Berry, J. A.: On the relationship between carbon isotope discrimination and the inter-cellular carbon dioxide concentration in leaves, Australian Journal of Plant Physiology, 9, 121-137, doi: 10.1071/PP9820121, 1982.

Fawcett, S. E., M. W. Lomas, J. R. Casey, B. B. Ward, and D. M. Sigman, Assimilation of upwelled nitrate by small eukaryotes in the Sargasso Sea, Nat. Geosci., 4, 717, doi: 10.1038/ngeo1265, 2011.

Finkel, Z. V., Beardall, J., Flynn, K. J., Quigg, A., Rees, T. A. V., and Raven, J. A., Phytoplankton in a changing world: cell size and elemental stoichiometry, Journal of Plankton Research, 32, 119-137, doi: 10.1093/plankt/fbp098 , 2010.

Fontugne, M., and J. C. Duplessy, Carbon isotope ratio of marine plankton related to surface water masses, Ear. Plan. Sci. Let., 41, 365-371, doi: 10.1016/0012-821x(78)90191-7, 1978.

Francey, R. J., Allison, C. E., Etheridge, D. M., Trudinger, C. M. , Enting, I. G., Leuenberger, M., Langenfelds, R. L., Michel, E., and Steele, L. P.: A 1000-year high precision record of delta C-13 in atmospheric CO2, Tellus Series B-Chemical and Physical Meteorology, 51, 170-193, doi:10.1034/j.1600-0889.1999.t01-1-00005.x, 1999.

Francois, R., M. A. Altabet, R. Goericke, D. C. McCorkle, C. Brunet, and A. Poisson.: Changes in the delta C-13 of surface water particulate organic matter across the subtropical convergence in the SW Indian Ocean, Global Biogeochemical Cycles., 7, 627-644, doi: 10.1029/93gb01277, 1993.

Freeman, K. H. and Hayes, J. M.: Fractionation of carbon isotopes by phytoplankton and estimates of ancient CO2 levels, Global Biogeochemical Cycles, 6, 185-198, 1992.

Friedli, H., Lotscher, H., Oeschger, H., Siegenthaler, U., and Stauffer, B.: Ice core record of the C-13/C-12 ratio of atmospheric CO_2 in the past two centuries, Nature, 324, 237-238, doi: 10.1038/324237a0, 1986.

Ganeshram, R. S., Calvert, S. E., Pedersen, T. F., and Cowie, G. L.: Factors controlling the burial of organic carbon in laminated and bioturbated sediments off NW Mexico: Implications for hydrocarbon preservation, Geochimica Et Cosmochimica Acta, 63, 1723-1734, 1999.

Gibb, S. W., Barlow, R. G., Cummings, D. G., Rees, N. W., Trees, C. C., Holligan, P., and Suggett, D.: Surface phytoplankton pig- ment distributions in the Atlantic Ocean: an assessment of basin scale variability between 50 degrees N and 50 degrees S, Prog. Oceanogr., 45, 339–368, doi: 10.1016/S0079-6611(00)00007-0, 2000.

Goericke, R., and Fry, B.: Variations of marine plankton delta C-13 with latitude, temperaure and dissolved CO_2 in the world ocean, Global Biogeochemical Cycles, 8, 85-90, doi:10.1029/93gb03272, 1994.

Gruber, N., Keeling, C. D., Bacastow, R. B., Guenther, P. R., Lueker, T. J. , Wahlen, M., Meijer, H. A. J., Mook, W. G. and Stocker, T. F., Spatiotemporal patterns of carbon-13 in the global surface oceans and the oceanic Suess effect, Global Biogeochemical Cy., 13, 307-335, doi:10.1029/1999gb900019, 1999.

Gruber, N., Clement, D., Carter, B. R., Feely, R. A., Heuven, S. van, Hoppema, M., Ishii, M., Key, R. M., Kozyr, A., Lauvset, S. K., Monaco, C. L., Mathis, J. T., Murata, A., Olsen, A., Perez, F. F., Sabine, C. L., Tanhua, T. and Wanninkhof, R.: The oceanic sink for anthropogenic CO_2 from 1994 to 2007, Science, 363, 1193–1199, doi:10.1126/science.aau5153, 2019.

5   Hansman, R. L. and Sessions, A. L.: Measuring the in situ carbon isotopic composition of distinct marine plankton populations sorted by flow cytometry, Limnology and Oceanography-Methods, 14, 87-99, 2016.

Hayes, J. M., Popp, B. N., Takigiku, R., and Johnson, M. W.: An isotopic study of biogeochemical relationships between carbonates and organic carbon in the Greenhorn formation, Geochimica Et Cosmochimica Acta, 53, 2961-2972,
10   doi:10.1016/0016-7037(89)90172-5, 1989.

Heimann, M., and Maier-Reimer, E.: On the relations between the oceanic uptake of CO_2 and its carbon isotopes. Global Biogeochemical. Cy. 10, 89–110. doi:10.1029/95GB03191, 1996.

15   Henley, S. F., Annett, A. L., Ganeshram, R. S., Carson, D. S., Weston, K., Crosta, X., Tait, A., Dougans, J., Fallick, A. E., and Clarke, A.: Factors influencing the stable carbon isotopic composition of suspended and sinking organic matter in the coastal Antarctic sea ice environment, Biogeosciences, 9, 1137-1157, doi:10.5194/bg-9-1137-2012, 2012.

Henson, S. A., Cole, H. S., Hopkins, J., Martin, A. P., and Yool, A.: Detection of climate change-driven trends in phytoplankton
20   phenology, Global Change Biology, 24, 101-111, doi:10.1111/gcb.13886, 2018.

Hofmann, M., Wolf-Gladrow, D. A., Takahashi, T., Sutherland, S. C., Six, K. D., and Maier-Reimer, E.: Stable carbon isotope distribution of particulate organic matter in the ocean: a model study, Mar. Chem., 72, 131-150, doi: 10.1016/s0304-4203(00)00078-5, 2000.
25
Humphreys, M. P., "Calculating seawater total alkalinity from open-cell titration data using a modified Gran plot technique," in Measurements and Concepts in Marine Carbonate Chemistry (PhD Thesis, Ocean and Earth Science, University of Southampton, UK), 25–44, 2015.

30   Humphreys, M. P.: Climate sensitivity and the rate of ocean acidification: future impacts, and implications for experimental design. ICES J. Mar. Sci. 74, 934–940. doi:10.1093/icesjms/fsw189, 2017.

Irwin, A. J. and Oliver, M. J.: Are ocean deserts getting larger?, Geophysical Research Letters, 36, 2009.

Jasper, J. P., Hayes, J. M. , Mix, A. C. , and Prahl, F. G.: Photosynthetic fractionation of C-13 and concentrations of dissolved CO2 in the central equatorial Pacific during the last 255,000 years, Paleoceanography, 9, 781-798, doi:10.1029/94pa02116, 1994.

5   Jasper, J. P. and Gagosian, R. B.: The sources and deposition of organic matter in the late quaternary pygmy basin, Gulf of Mexico, Geochimica Et Cosmochimica Acta, 54, 1117-1132, 1990.

Keeling, C. D.: The Suess effect: [13]Carbon-[14]Carbon interrelations. Environ. Int. 2, 229–300, doi: 10.1016/0160-4120(79)90005-9, 1979.

Khatiwala, S., Tanhua, T., Mikaloff Fletcher, S., Gerber, M., Doney, S. C., Graven, H. D., Gruber, N., McKinley, G. A., Murata, A., Ríos, A. F., and Sabine, C. L.: Global ocean storage of anthropogenic carbon, Biogeosciences, 10, 2169-2191, doi: 10.5194/bg-10-2169-2013, 2013.

15   Latasa, M., and Bidigare, R. R.: A comparison of phytoplankton populations of the Arabian Sea during the Spring Intermonsoon and Southwest Monsoon of 1995 as described by HPLC-analyzed pigments, Deep-Sea Res. Pt. I, 45, 2133-2170, 1998.

Laws, E. A., Popp, B. N., Bidigare, R. R., Kennicutt, M. C., and Macko, S. A., Dependence of phytoplankton carbo isotopic
20   composition on growth rate and CO2(aq) – Theoretical considerations and experimental results, Geochimica Et Cosmochimica Acta, 59, 1131-1138, doi:10.1016/0016-7037(95)00030-4, 1995.

Lee, K., Kim, T.-W., Byrne, R. H., Millero, F. J., Feely, R. A., and Liu, Y.-M.: The universal ratio of boron to chlorinity for the North Pacific and North Atlantic oceans. Geochim. Cosmochim. Acta 74, 1801–1811. doi:10.1016/j.gca.2009.12.027,
25   2010.

Le Quere, C., Aumont, O., Bopp, L., Bousquet, P., Ciais, P., Francey, R., Heimann, M., Keeling, C. D., Keeling, R. F., Kheshgi, H., Peylin, P., Piper, S. C., Prentice, I. C., and Rayner, P. J.: Two decades of ocean CO2 sink and variability, Tellus Series B-Chemical and Physical Meteorology, 55, 649-656, 2003.

Lewis, E., and Wallace, D. W. R.: Program Developed for CO_2 System Calculations. ORNL/CDIAC-105, Carbon Dioxide Information Analysis Center, Oak Ridge National Laboratory, U.S. Department of Energy, Oak Ridge, TN, USA, 1998.

Lindell, D., and Post, A. F.: Ultraphytoplankton succession is triggered by deep winter mixing in the Gulf of Aqaba (Eilat), Red Sea, Limnol. Oceanogr., 40, 1130-1141, doi: 10.4319/lo.1995.40.6.1130, 1995.

Lourey, M. J., Trull, T. W., and Tilbrook, B.: Sensitivity of delta C-13 of Southern Ocean suspended and sinking organic matter to temperature, nutrient utilization, and atmospheric CO2, Deep-Sea Res. Pt. I, 51, 281-305, doi:10.1016/j.dsr.2003.10.002, 2004.

Maranon, E., Lorenzo, M. P., Cermeno, P., and Mourino-Carballido, B.: Nutrient limitation suppresses the temperature dependence of phytoplankton metabolic rates, Isme Journal, 12, 1836-1845, doi: 10.1038/s41396-018-0105-1, 2018.

McNeil, B. I., Matear, R. J., and Tilbrook, B.: Does carbon 13 track anthropogenic CO_2 in the Southern Ocean? Global Biogeochem. Cycles, 15, 597–613. doi:10.1029/2000GB001352, 2001.

Mehrbach, C., Culberson, C. H., Hawley, J. E., and Pytkowicz, R. M.: Measurement of the Apparent Dissociation Constants of Carbonic Acid in Seawater at Atmospheric Pressure. Limnol. Oceanogr. 18, 897–907. doi:10.4319/lo.1973.18.6.0897, 1973.

Middelburg, J. J.: Stable isotopes dissect aquatic food webs from the top to the bottom, Biogeosciences, 11, 2357-2371, https://doi.org/10.5194/bg-11-2357-2014, 2014.

Minagawa, M. and Wada, E.: Stepwise Enrichment of N-15 Along Food-Chains – further Evidence and the Relation between DeltaN-15 and Animal Age, Geochimica Et Cosmochimica Acta, 48, 1135–1140, doi:10.1016/0016-7037(84)90204-7, 1984.

Pancost, R. D., Freeman, K. H., Wakeham, S. G., and Robertson, C. Y.: Controls on carbon isotope fractionation by diatoms in the Peru upwelling region, Geochimica Et Cosmochimica Acta, 61, 4983-4991, 1997.

Peterson, B. J. and Fry, B.: Stable isotopes in ecosystem studies, Annual Review of Ecology and Systematics, 18, 293-320, 1987.

Popp, B. N., Laws, E. A., Bidigare, R. R., Dore, J. E., Hanson, K. L., and Wakeham, S. G.: Effect of phytoplankton cell geometry on carbon isotopic fractionation, Geochimica Et Cosmochimica Acta, 62, 69-77, doi:10.1016/s0016-7037(97)00333-5, 1998.

Popp, B. N., et al..: Controls on the carbon isotopic composition of Southern Ocean phytoplankton, Global Biogeochemical Cycles., 13, 827-843, doi: 10.1029/1999gb900041, 1999.

Quay, P., Sonnerup, R., Westby, T., Stutsman, J., and McNichol, A.: Changes in the C-13/C-12 of dissolved inorganic carbon in the ocean as a tracer of anthropogenic CO2 uptake, Global Biogeochemical Cycles., 17, doi:10.1029/2001gb001817, 2003.

5   Rau, G. H., Teyssie, J. L., Rassoulzadegan, F., and Fowler, S. W.: C-13/C-12 and N-15/N-14 variations among size-fractionated marine particles – implications for their origin and trophic relationships, Mar. Ecol. Prog. Ser., 59, 33-38, 1990.

Rau, G. H., Froelich, P. N., Takahashi, T., and Des Marais, D. J.: Does sedimentary organic d13C record variations in quaternary ocean CO2aq?, Paleoceanography, 6, 335-347, doi:10.1029/91pa00321, 1991.

Rau, G. H., Riebesell, U., and Wolf-Gladrow, D.: A model of photosynthetic C-13 fractionation by marine phytoplankton based on diffusive molecular CO_2 uptake, Mar. Ecol. Prog. Ser., 133, 275-285, doi: 10.3354/meps133275, 1996.

Rau, G. H., Takahashi, T., and Marais, D. J. D., Latitudinal variations in plankton delta C-13 – implications for CO2 and

15   productivity in past oceans, Nature, 341, 516-518, doi:10.1038/341516a0, 1989.

Raven, J. A., Cockell, C. S., and La Rocha, C. L.: The evolution of inorganic carbon concentrating mechanisms in photosynthesis, Philosophical Transactions of the Royal Society B-Biological Sciences, 363, 2641-2650, doi:10.1098/rstb.2008.0020, 2008.

Rousseaux, C. S., and W. W. Gregg.: Recent decadal trends in global phytoplankton composition, Global Biogeochem. Cycles, 29, 1674–1688, doi: 10.1002/2015GB005139, 2015.

Sabine, C. L., and Tanhua, T.: Estimation of Anthropogenic CO2 Inventories in the Ocean, Ann. Rev. Mar. Sci., 2, 175-198, ,

25   doi: 10.1146/annurev-marine-120308-080947, 2010.

Sackett, W. M.: The depositional history and isotopic organic carbon composition of marine sediments, Marine Geology, 2, 173-185, 1964.

30   Sackett, W. M., Eckelmann, W. R., Bender, M. L., and Be, A. W. H.: Temperature dependence of carbon isotope composition in marine plankton and sediments, Science, 148, 235-+, doi:10.1126/science.148.3667.235, 1965.

Sarmiento, J. L., Slater, R., Barber, R., Bopp, L., Doney, S. C., Hirst, A. C., Kleypas, J., Matear, R., Mikolajewicz, U., Monfray, P., Soldatov, V., Spall, S. A., and Stouffer, R.: Response of ocean ecosystems to climate warming, Global Biogeochemical Cycles., 18, GB3003, doi:10.1029/2003gb002134, 2004.

5   Schlitzer, R., Ocean Data View, odv.awi.de, 2018.

Sharkey, T. D., Berry, J. A., and Raschke, K.: Starch and sucrose synthesis in phaeseolus-vulgaris as affected by light, CO2 and abscisic acid, Plant Physiology, 77, 617-620, 1985.

10   Siegel, D. A., S. Maritorena, N. B. Nelson, M. J. Behrenfeld, and C. R. McClain, Colored dissolved organic matter and its influence on the satellite-based characterization of the ocean biosphere, Geophys. Res. Lett., 32, L20605, doi: 10.1029/2005gl024310, 2005.

Stocker, T. F., Qin, D., Plattner, G.-K., Alexander, L. V., Allen, S. K., Bindoff, N. L., et al.: "Technical Summary," in Climate
15   Change 2013: The Physical Science Basis. Contribution of Working Group I to the Fifth Assessment Report of the Intergovernmental Panel on Climate Change, eds. T. F. Stocker, D. Qin, G.-K. Plattner, M. Tignor, S. K. Allen, J. Boschung, et al. (Cambridge, United Kingdom and New York, NY, USA: Cambridge University Press), 33–115. Available at: www.climatechange2013.org, 2013.

20   Tuerena, R. E., Ganeshram, R. S., Geibert, W. Fallick, A. E., Dougans, J., Tait, A., Henley, S. F., Woodward, E. M. S.: Nutrient cycling in the Atlantic basin: The evolution of nitrate isotope signatures in water masses, Global Biogeochemical Cycles., 29, 1830-1844, doi.org/10.1002/2015GB005164, 2015.

Uitz, J., Huot, Y., Bruyant, F., Babin, M., and Claustre, H.: Relating phytoplankton photophysiological properties to
25   community structure on large scales, Limnol. Oceanogr., 53, 614-630, doi:10.4319/lo.2008.53.2.0614, 2008.

van Heuven, S., Pierrot, D., Rae, J. W. B., Lewis, E., and Wallace, D. W. R.: CO2SYS v 1.1, MATLAB program developed for CO2 system calculations. ORNL/CDIAC-105b, Carbon Dioxide Information Analysis Center, Oak Ridge National Laboratory, U.S. Department of Energy, Oak Ridge, TN, USA. doi:10.3334/CDIAC/otg.CO2SYS_MATLAB_v1.1, 2011.

Villinski, J. C., Dunbar, R. B., and Mucciarone, D. A.: Carbon 13 Carbon 12 ratios of sedimentary organic matter from the Ross Sea, Antarctica: A record of phytoplankton bloom dynamics, J. Geophys. Res. Oceans, 105, 14163-14172, doi: 10.1029/1999jc000309, 2000.

Weiss, R. F. : Carbon dioxide in water and seawater: the solubility of a non-ideal gas. Marine Chemistry. 2, 203-215, doi: 10.1016/0304-4203(74)90015-2, 1974.

Young, J. N., Bruggeman, J., Rickaby, R. E. M., Erez, J., and Conte, M.: Evidence for changes in carbon isotopic fractionation by phytoplankton between 1960 and 2010, Global Biogeochemical Cycles., 27, 505-515, doi:10.1002/gbc.20045, 2013.

Zeebe, R. E., Sanyal, A., Ortiz, J. D., and Wolf-Gladrow, D. A.: A theoretical study of the kinetics of the boric acid-borate equilibrium in seawater, Marine Chemistry, 73, 113-124, 2001.
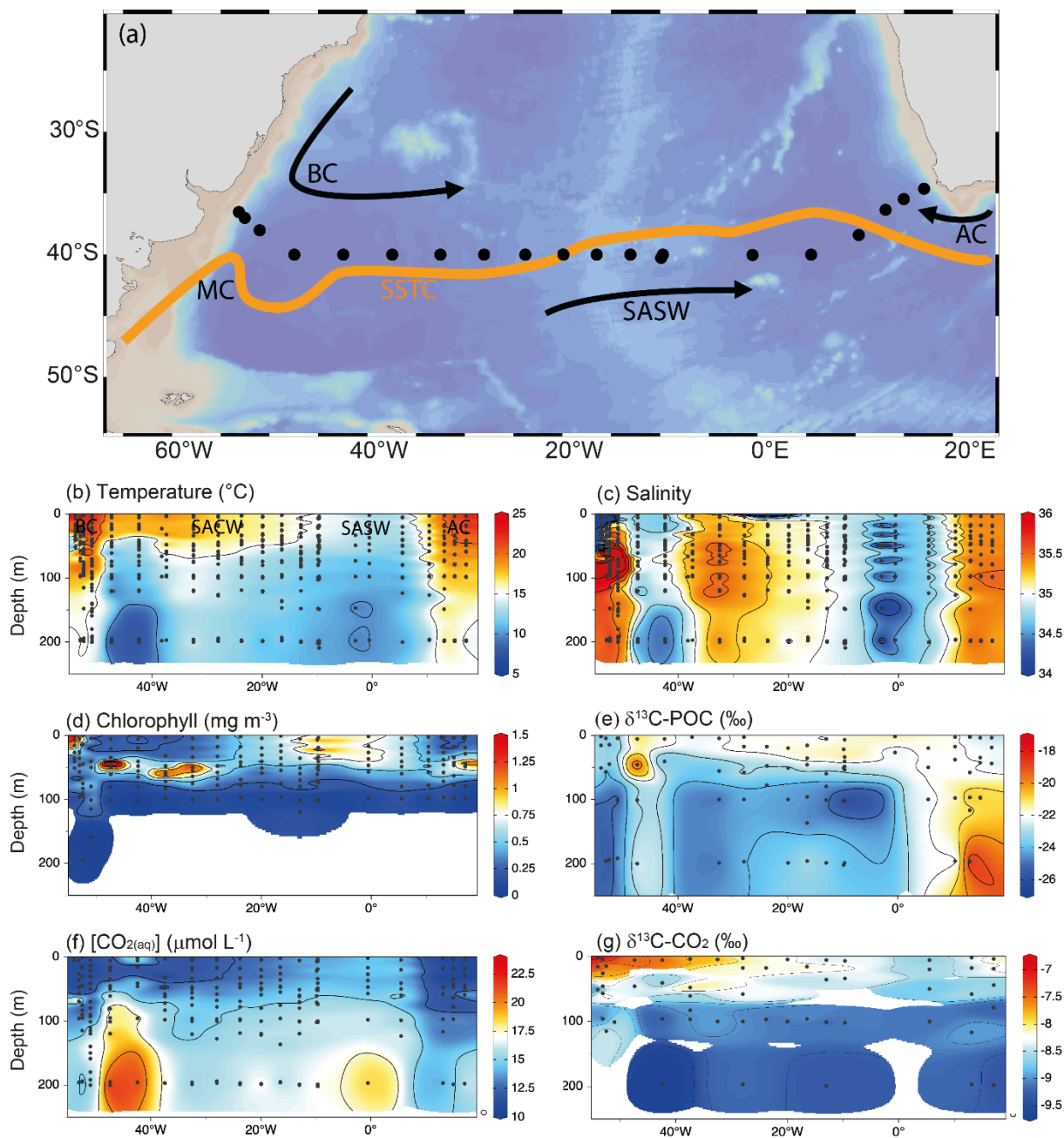
Figure 1. Map and longitudinal transects across the south subtropical convergence. (a) Map of study region, the orange line depicts the subtropical front (SST=16°C, from Browning et al., 2014). Longitudinal transects of (b) temperature, (c) Salinity, (d) Chlorophyll, (e) $\delta^{13}C_{POC}$, (f) $[CO_{2(aq)}]$, and (g) $\delta^{13}C_{CO2}$ in the upper 250 m. The water masses are identified in (b), BC=Brazil Current, SACW=South Atlantic Central Water, SASW=Subantarctic Surface Water, AC=Agulhas Current. The interpolation in b-g was produced using ODV-weighted average gridding (Schlitzer, 2018).
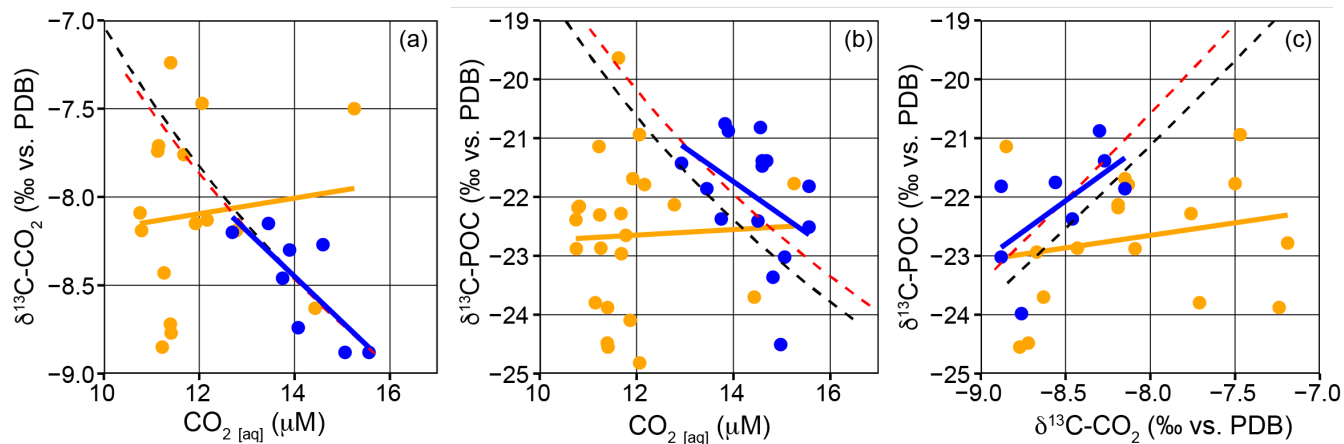
Figure 2. Correlations between [CO$_{2(aq)}$], δ^{13}C$_{POC}$, and δ^{13}C$_{CO2}$ in surface waters. (a) δ^{13}C$_{CO2}$ versus [CO$_{2(aq)}$], (b) δ^{13}C$_{POC}$ versus [CO$_{2(aq)}$], (c) δ^{13}C$_{POC}$ versus δ^{13}C$_{CO2}$. Blue points represent SASW samples and orange points represent subtropical samples. A linear regression for each region is shown in the respective colour, all regressions were insignificant (p>0.05), apart from SASW samples in (a) where r=-0.77, n=12, p=0.003. The dashed line displays the expected trend due to diffusive uptake of carbon by phytoplankton using temperature and not cell size, red= atmospheric CO$_2$ 350ppm, 1.7 ‰, (Rau et al., 1996), black= 390ppm, 1.3 ‰ (representative of this study).
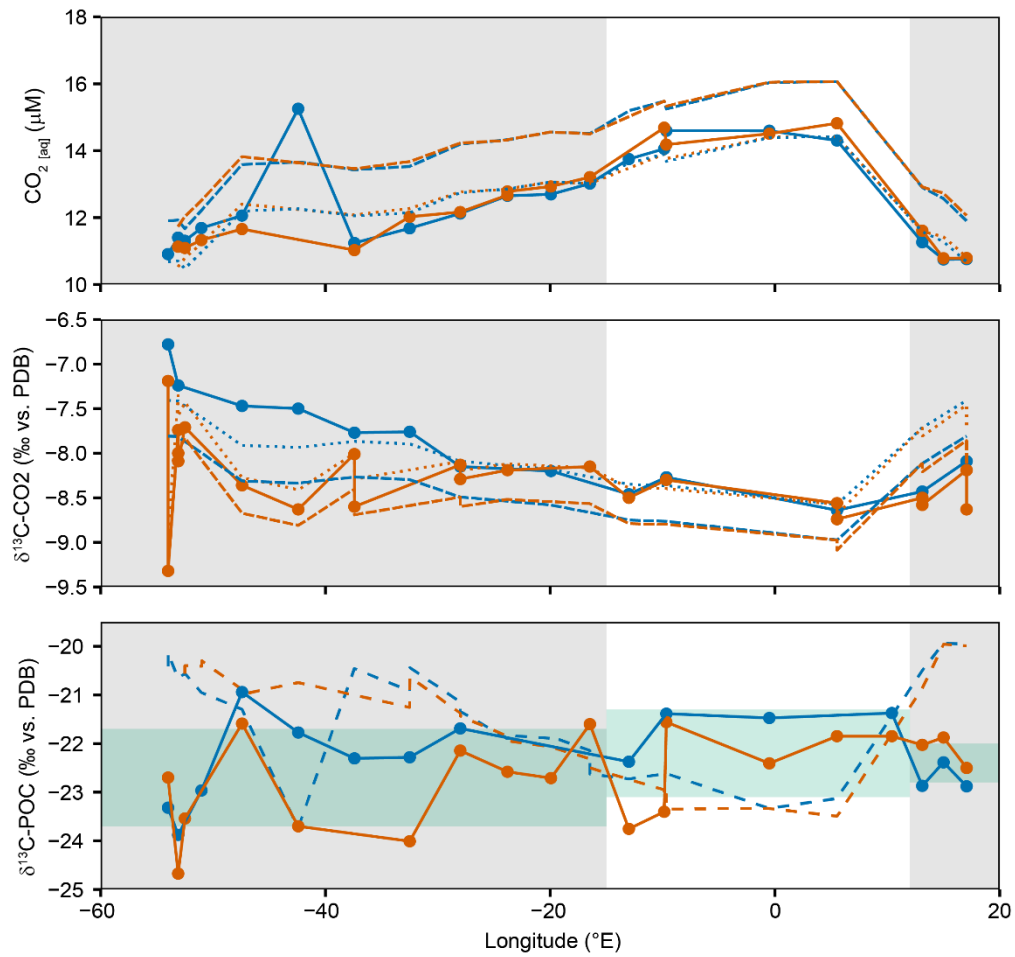
Figure 3. Distribution of (a) [CO$_{2(aq)}$] (b) δ^{13}C$_{CO2}$ and (c) δ^{13}C$_{POC}$, versus longitude. Closed circles and solid lines show measured values and trends. Orange lines and points = 5 m, Blue lines and points = 20 m. In (a) and (b), Dashed lines are modelled estimates using temperature only (Rau et al., 1996). Long dash: atmospheric CO$_2$ = 390ppm, dotted line atmospheric CO$_2$ =350ppm. In (c) Dashed lines are modelled estimates using temperature, [CO$_{2(aq)}$] and δ^{13}C$_{CO2}$. Grey shaded areas highlight the stations sampled north of the SSTC. Green shaded bars represent 2σ for SACW, SASW and AC regions of the transect.
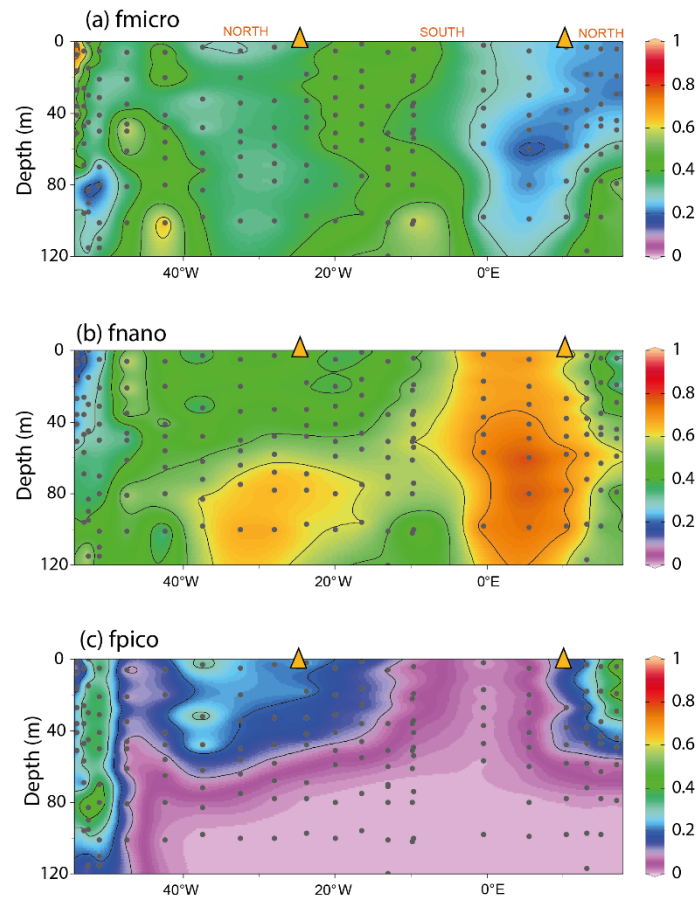
Figure 4. The fractional contribution of phytoplankton size classes to total chlorophyll as estimated from phytoplankton pigments. The size classes are defined as pico < 2 μm, nano = 2 – 20 μm and micro = 20 – 200 μm. 'f' signifies fractional contribution to chlorophyll-a concentration. Size class estimates were calculated following (Uitz et al., 2008). The interpolation was produced using ODV-weighted average gridding (Schlitzer, 2018).
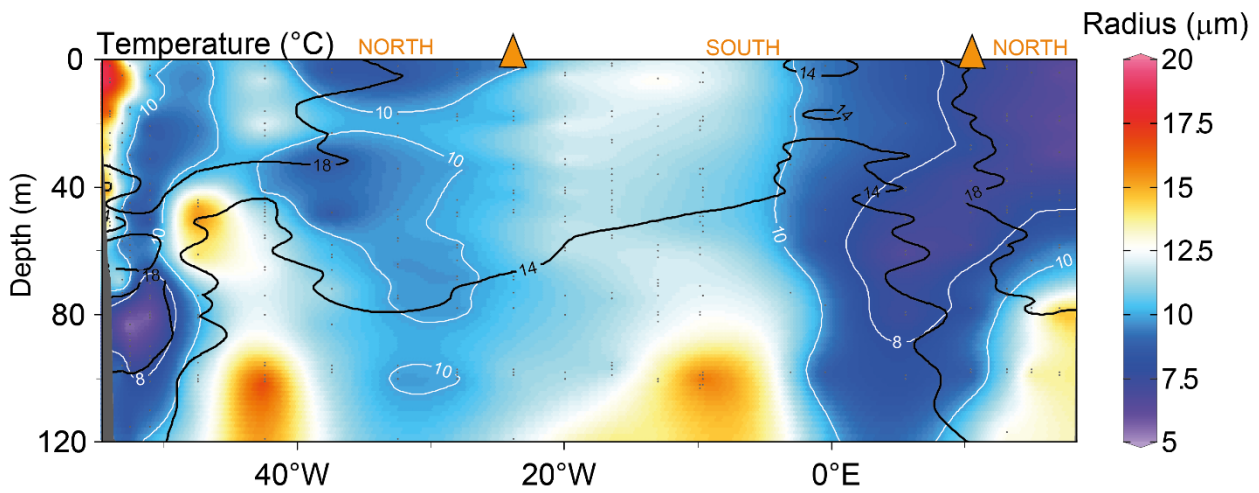
Figure 5. The estimated average phytoplankton community cell radius. The average radius (white contour lines) was calculated using the proportions of pico-, nano- and microplankton in Figure 4. We estimate the average radius using assumed cellular radii of 0.5, 2.5 and 25 μm for pico-, nano- and microplankton, respectively. The black contour lines show the 14°C and 18°C isotherms. The interpolation was produced using ODV-weighted average gridding (Schlitzer, 2018).
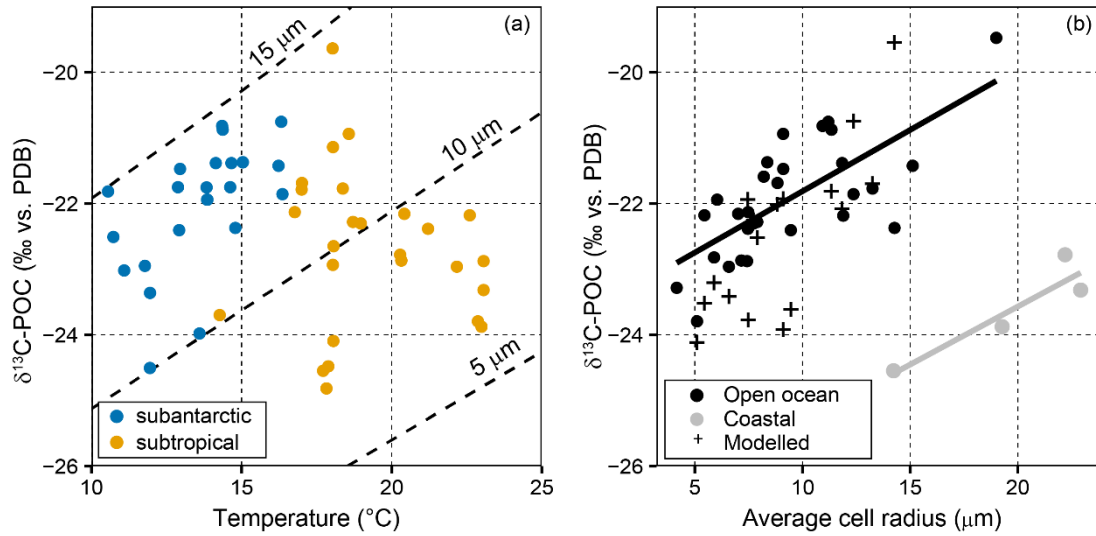
Figure 6. $\delta^{13}C_{POC}$ variability and model predictions with temperature and cell size. (a) $\delta^{13}C_{POC}$ versus temperature, with the modelled estimates for cell radii of 5, 10 and 15 µm. Blue circles = SASW, orange circles = subtropical waters. (b) $\delta^{13}C_{POC}$ vs cell radius as derived from pigment data. Samples from the eastern and western margin are excluded from correlation estimates. Rio Plata: r=0.92, df=2, p=0.075; Open ocean: r=0.72, df=30, p<0.001. Modelled $\delta^{13}C_{POC}$ is estimated using measured temperature and cell size and an assumed constant cell growth rate of 1.1 d^{-1}. Black crosses show modelled results. Average cell radius calculated from micro-plankton (25 µm), nano-plankton (2.5 µm) and pico-plankton (0.5 µm). There are less data in (b) as we did not have corresponding cell size data for all of the $\delta^{13}C_{POC}$ measurements.
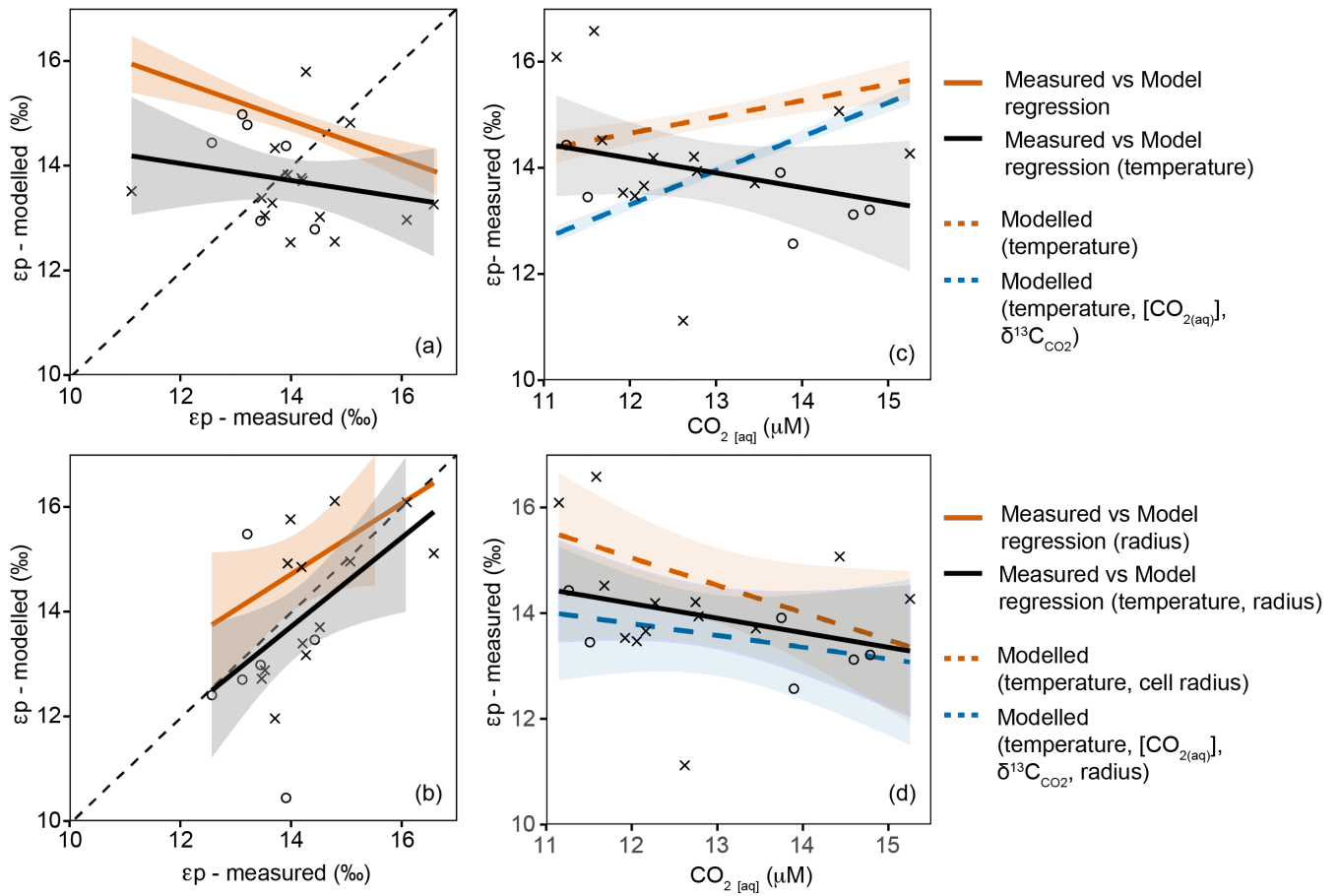
Figure 7. Variation in modelled and measured ε_p in the upper 60m with changing [CO$_{2(aq)}$]. Black points and lines show measured ε_p, circles = SASW, crosses = subtropical water masses. (a) and (c) the regressions for modelled and measured ε_p, (b) and (d) modelled and measured ε_p against [CO$_{2(aq)}$]. The top panel explores the predicted ε_p using temperature, [CO$_{2(aq)}$] and $\delta^{13}C_{CO2}$. The bottom panel explores the predicted ε_p using temperature, [CO$_{2(aq)}$], $\delta^{13}C_{CO2}$ and cell size.
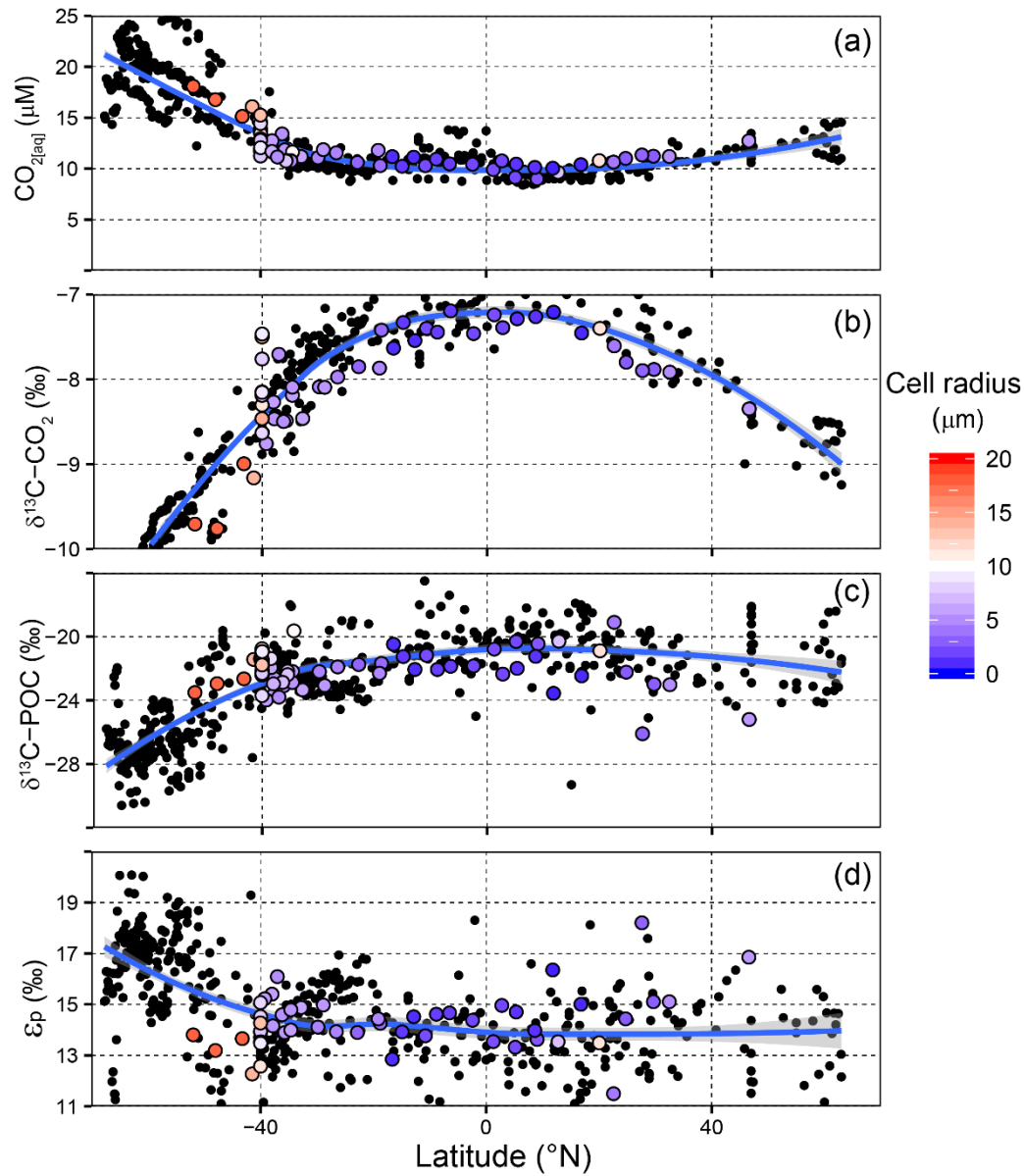
Figure 8. Global distributions of (a) [CO$_{2(aq)}$], (b) δ^{13}C$_{CO2}$, (c) δ^{13}C$_{POC}$ and (d) ε$_p$ in surface waters, plotted against latitude. Data include samples from δ^{13}C$_{POC}$ compilation in Young et al., 2013 and data from this study. Coloured points show cell radius estimates (AMT3, AMT18 and this study). Blue lines in each show a loess fitted curve for the dataset.
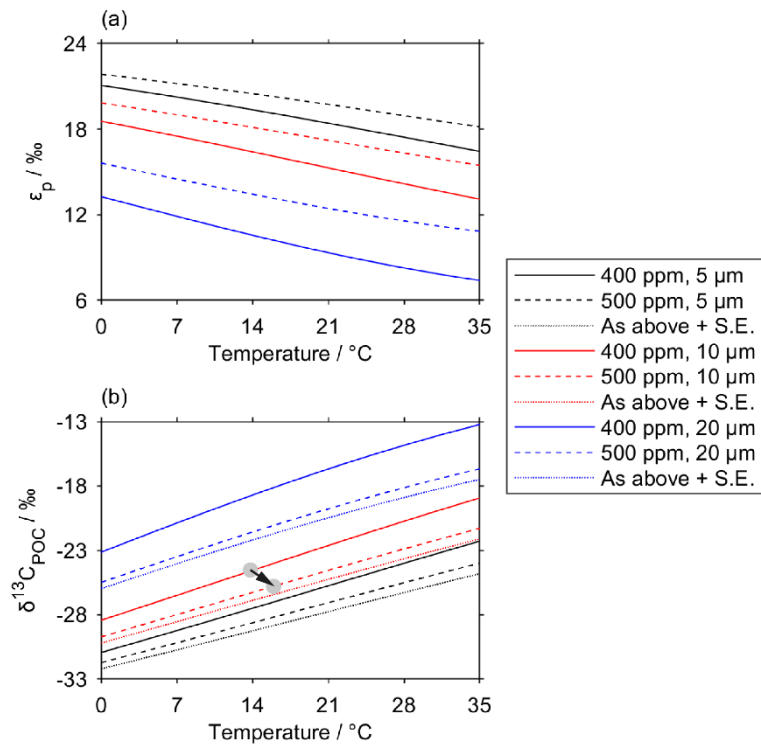
Figure 9. Projected changes in ε_p and $\delta^{13}C_{POC}$ due to ongoing anthropogenic emission and upper ocean uptake of CO_2 for different temperatures and cell sizes. Variation in ε_p with seawater temperature for CO_2 partial pressures of 400 ppm (solid line) and 500 ppm (dashed line) and average community cell radii of 5 µm (black), 10 µm (red) and 20 µm (blue). (b) Variation in $\delta^{13}C_{POC}$ under the same conditions as in (a), also showing the additional isotopic change driven by the Suess effect (labelled "S.E.", dotted lines). $CO_{2(aq)}$ is calculated using the atmospheric CO_2 concentration and the solubility of CO_2 in seawater (Weiss, 1974). The arrow in (b) indicates how 100ppm increase in CO2 and a projected 2C increase in temperature would impact d13C (with no change in cell size).